4-5-2023

Inorganic carbon outwelling from a Mediterranean seagrass meadow using radium isotopes

Claudia Majtényi-Hill

Gloria Reithmaier

Yvonne Y. Y. Yau

Oscar Serrano
Edith Cowan University

Nerea Piñeiro-Juncal

See next page for additional authors

10.1016/j.ecss.2023.108248

Majtényi-Hill, C., Reithmaier, G., Yau, Y. Y., Serrano, O., Piñeiro-Juncal, N., & Santos, I. R. (2023). Inorganic carbon outwelling from a Mediterranean seagrass meadow using radium isotopes. Estuarine, *Coastal and Shelf Science*, 283, Article 108248.
https://doi.org/10.1016/j.ecss.2023.108248

Estuarine, Coastal and Shelf Science 283 (2023) 108248

Contents lists available at ScienceDirect

Estuarine, Coastal and Shelf Science

journal homepage: www.elsevier.com/locate/ecss

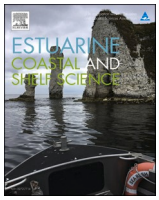

Inorganic carbon outwelling from a Mediterranean seagrass meadow using radium isotopes

Claudia Majtényi-Hill [a,*], Gloria Reithmaier [a], Yvonne Y.Y. Yau [a], Oscar Serrano [b,c], Nerea Piñeiro-Juncal [b,d,e], Isaac R. Santos [a]

[a] Department of Marine Sciences, University of Gothenburg, Sweden
[b] Centro de Estudios Avanzados de Blanes, Consejo Superior de Investigaciones Científicas, Blanes, Spain
[c] School of Science and Centre for Marine Ecosystems Research, Edith Cowan University, Joondalup, WA, Australia
[d] Department of Biology & CESAM – Centre for Environmental and Marine Studies, University of Aveiro, Aveiro, Portugal
[e] CRETUS, EcoPast (GI-1553), Facultade de Bioloxía, Universidade de Santiago de Compostela, Campus Sur s/n, Santiago de Compostela, 15782, Spain

ARTICLE INFO

Keywords:
Blue carbon
Carbon cycle
Flux
Emissions
Posidonia oceanica
Climate change

ABSTRACT

Seagrass meadows are 'blue carbon' ecosystems widely recognised for their potential role in climate change mitigation. Previous studies have focused mainly on carbon storage within meadows and sediments. However, little is known about contribution of outwelling (i.e., lateral transport) to seagrass carbon budgets. Here, radium isotopes (^{223}Ra and ^{224}Ra) were used to assess dissolved inorganic carbon (DIC) and total alkalinity (TA) outwelling from a Mediterranean *Posidonia oceanica* meadow during early autumn. DIC outwelling was 114 ± 61 mmol m^{-2} day^{-1} and exceeded above-meadow CO_2 outgassing (3 ± 1 mmol m^{-2} day^{-1}). Production of DIC was uncoupled from TA and fuelled by net heterotrophy and aerobic processes within the meadow. The small export of TA (5 ± 6 mmol m^{-2} day^{-1}) implied that ~90% of outwelled DIC may return to the atmosphere as CO_2 in offshore waters. Combining these fluxes with above-meadow outgassing suggested a total carbon loss that exceeded long term burial in sediments. Overall, the meadow acted as a carbon source to the atmosphere during the early autumn season. Further studies quantifying outwelling at multiple spatial and temporal scales are required to better resolve seagrass carbon budgets and their contribution to carbon sequestration.

1. Introduction

The term 'blue carbon' is often used to describe the carbon sequestration function of vegetated coastal zones (Nelleman et al., 2008). Among this suite of ecosystems are seagrass meadows, which sequester ~20% of total carbon buried in the ocean despite covering just 0.1% of surface area (Duarte et al., 2013). Seagrass area, however, is decreasing at an alarming rate. A net loss of 5602 km^2 has been experienced globally during the last century, with a decline of ~10% in the Mediterranean (Dunic et al., 2021). Attention has therefore focused on preservation and restoration, as well as development of schemes using seagrass for climate change mitigation (Macreadie et al., 2017; Maxwell et al., 2017). For these management efforts to be effective, it is vital that understanding of carbon budgets is improved (Macreadie et al., 2019; Mcleod et al., 2011; Ruiz Fernandez et al., 2009).

Seagrasses meet the 'blue carbon' criteria due to their ability to sequester large amounts of carbon in sediments on millennial timescales. This is derived from a combination of high metabolic capacity and effective sediment storage (Duarte et al., 2013). Globally, 63% of seagrass sites are net autotrophic, with an average production-to-respiration ratio of 1.55 (Duarte et al., 2010). Photosynthetic production of above and below ground biomass removes dissolved inorganic carbon (DIC) from the water column. Trapping of allochthonous particles and slow decomposition of recalcitrant root structures further enhances carbon accumulation, creating sediment deposits several metres thick (Duarte et al., 2010; Fourqurean et al., 2012; Serrano et al., 2012). However, mineralisation processes decompose organic matter, thereby generating DIC. Calcification and carbonate dissolution also drive DIC consumption and production at some seagrass sites (Barrón et al., 2006; Champenois and Borges, 2021; Van Dam et al., 2021b). Ultimately, the DIC produced may interact with the overlying atmosphere via gas exchange (Santos et al., 2021).

Previous studies have focused mainly on processes within meadows when evaluating overall carbon sequestration. However, outwelling

* Corresponding author.
E-mail address: cloudymajtenyihill@gmail.com (C. Majtényi-Hill).

https://doi.org/10.1016/j.ecss.2023.108248
Received 27 October 2022; Received in revised form 23 January 2023; Accepted 27 January 2023
Available online 31 January 2023

(lateral transport across the shelf) has recently gained attention (Santos et al., 2021). Due to carbon speciation and varying fates following export, outwelling can either enhance or detract from meadow sequestration (Duarte and Krause-Jensen, 2017; Santos et al., 2021). It is therefore essential to consider outwelling within seagrass carbon budgets. In the Mediterranean Sea, outwelling of organic carbon may represent 79% of seagrass net primary production (Champenois and Borges, 2021). This typically occurs episodically following seasonal patterns of water temperature, leaf senescence and wave action associated with storms (Barrón et al., 2014; Mateo and Romero, 1997). Of this exported material, 14% of POC and 33% of DOC may escape remineralisation and accumulate in the deep ocean on timescales relevant to climate change mitigation (Duarte and Krause-Jensen, 2017). DIC can also follow the outwelling path in seagrass meadows, but has yet to be quantified despite being the largest carbon pool in the ocean (Cole et al., 2021; Santos et al., 2021).

The fate of outwelled DIC is intrinsically linked to the carbonate system and its relationship to total alkalinity (TA) (Ismail, 2021). DIC corresponds to the sum of three carbon species ($[CO_2]$ + $[HCO_3^-]$ + $[CO_3^{2-}]$) present in the ocean, whereas TA represents the capacity to neutralise hydrogen ions (Middelburg et al., 2020; Pimenta and Grear, 2018). In seagrass sediments, TA is generated from anaerobic processes (e.g., sulphate reduction and denitrification) and carbonate dissolution. Processes such as aerobic mineralisation and calcification consume TA (Barrón et al., 2006; Chou et al., 2018, 2021; Hu and Cai, 2011; Van Dam et al., 2021b). Ultimately, the fraction of DIC exported as TA determines whether DIC outwelling becomes a long-term sink or a short-term recycling mechanism for carbon (Santos et al., 2021). This is because CO_2 exchanges with the atmosphere (Middelburg et al., 2020), whereas carbonate alkalinity ($[HCO_3^-]$ + $[CO_3^{2-}]$) can reside in the ocean for ~100,000 years (Millero, 2007). When a source of TA is present, conversion of CO_2 to carbonate species is favoured. Outwelled carbonate alkalinity can therefore enter the deep oceanic pool. Alternatively, a lack of concurrent TA export creates opportunities for CO_2 atmospheric exchange (Burt et al., 2021; Maher et al., 2018).

Outwelling research has been restricted by challenges associated with quantification (Santos et al., 2021). Methods currently available include physical measurements, numerical modelling, mass balance budgets and tracer techniques (Champenois and Borges, 2021; Moore and de Oliveira, 2008). The use of radium isotopes offers a promising approach to quantifying outwelling fluxes. Radium isotopes desorb from sediment particles upon contact with seawater, thereby providing a naturally occurring tracer that is continually added to marine waters. Radium also behaves conservatively, meaning the only processes affecting its distribution in the ocean are mixing and decay (Charette et al., 2007). In particular, short-lived isotopes (^{223}Ra and ^{224}Ra) can resolve coastal mixing processes due to the appropriate timescales of their decay, enabling estimates of mixing rates and apparent water ages in coastal seawater (Moore, 2000a, 2000b). Other studies have applied radium isotopes for constraining DIC outwelling in mangrove and saltmarsh systems (Cabral et al., 2021; Tamborski et al., 2021), but not yet in seagrass meadows.

The aim of this study is to estimate DIC and TA outwelling from a Mediterranean seagrass meadow using radium isotopes. To put results in perspective, we performed a meadow timeseries to quantify net community production (NCP), a spatial survey in the bay to quantify CO_2 air-sea fluxes, and cross-shore transects of radium isotopes to quantify outwelling. We build on the seagrass literature by (1) focusing on outwelling rather than burial as a potential carbon sequestration pathway, and (2) focusing on inorganic rather than organic carbon as a product of seagrass metabolism.

2. Methods

2.1. Site description

This study was conducted along the Spanish coast of the northwest Mediterranean Sea in the bay of Portlligat (42°17′32″ N, 3°17′28 E″) (Fig. 1). Surface area of the bay reaches 0.11 km^2 (Lo Iacono et al., 2008), with water depths up to 14 m (GENCAT, 2000). The bay is semi-sheltered and connected to the sea by a 213 m wide opening in the northeast. Tides are minimal and range by just 0.2 m (ECMWF, 2022). A typical Mediterranean climate prevails, with September temperatures and precipitation averaging 20.6 °C and 0.18 cm h^{-1} during the past 30 years (Hersbach et al., 2018). Waters are clear, oligotrophic and oxygenated, providing optimal conditions for the growth of the endemic seagrass species *Posidonia oceanica* (Koopmans et al., 2018). In Portlligat, a dense meadow (>600 shoots m^{-2}) of *P. oceanica* dominates the seafloor, covering 41% of the total bay area. The remaining area is mostly occupied by dead seagrass and bare sand patches (Lo Iacono et al., 2008). Despite relatively slow growth rates, *P. oceanica* are known for substantial biomass both above and belowground (Barron and Duarte, 2009). This high production (54–119 mmol C m^{-2} day^{-1}) (Koopmans et al., 2020) coupled with the refractory nature of root tissues leads to the development of a characteristic 'matte', in which carbon accumulates with residence times longer than 10,000 years (Mateo et al., 2006). Local sediment cores and seismic surveys revealed a dense 6.2 m thick matte at Portlligat (Lo Iacono et al., 2008). Upper sediment layers contained abundant organic matter composed of roots, rhizomes and leaf sheaths. Organic matter content depleted in lower layers, whilst carbonate concentration increased (Serrano et al., 2012).

2.2. Meadow timeseries

Timeseries observations were performed at two locations within the meadow (~20 cm above seafloor) between 11th – 23rd September 2021. *Station 1* (42°17′38″ N, 3°17′19 E″) was situated in the north of the bay in an area of healthy dense seagrass, whilst *Station 2* (42°17′29″ N, 3°17′22 E″) was located toward the south in an interspersed zone with some dead seagrass patches (Fig. 1b). Submersible sensors provided continuous records of dissolved oxygen (DO) concentrations (miniDOT, PME) at 1 minute resolution, whilst conductivity, temperature and pressure (Levelogger 5 LTC, Solinst) were measured every 5 minutes. Climatic variables at hourly frequency were sourced from ERA5 reanalysis products (Hersbach et al., 2018).

Calculations of metabolic status were based on the integrative 'open-water' mass balance approach originally developed by Odum (1956) and widely used in shallow aquatic systems (Ganguly et al., 2017; Van Dam et al., 2019). This method defines NCP as the difference between 'gross primary production' (GPP) and 'respiration' (R) from the 'biological dissolved oxygen change' (BDO) over a 24-h period (Equation (1)). To account for effects of temperature and salinity, DO was converted to saturation percentage ($DO_{\%sat}$) prior to calculations (Needoba et al., 2012). In practice, BDO is the measured change in DO minus the non-biological influence of depth-integrated (h in m) air-sea gas exchange (F_{O2}) (Equation (2)). The gas exchange term was estimated using three different parameterisations (Ho et al., 2006; Nightingale et al., 2000; Wanninkhof and McGillis, 1999), resulting in final NCP given as a range with median, minimum and maximum estimations. Atmospheric value for O_2 was approximated as the saturation value at surface (Needoba et al., 2012). Final results for NCP were converted to units of carbon by assuming photosynthetic and respiratory quotients of 1 (Tokoro et al., 2014).

$$NCP = GPP - R = \Sigma BDO \quad (1)$$

$$BDO_t = (DO_t - DO_{t-1}) \times h - F_{O2} \quad (2)$$

Dividing NCP over a 24-h cycle into photo and dark periods allows

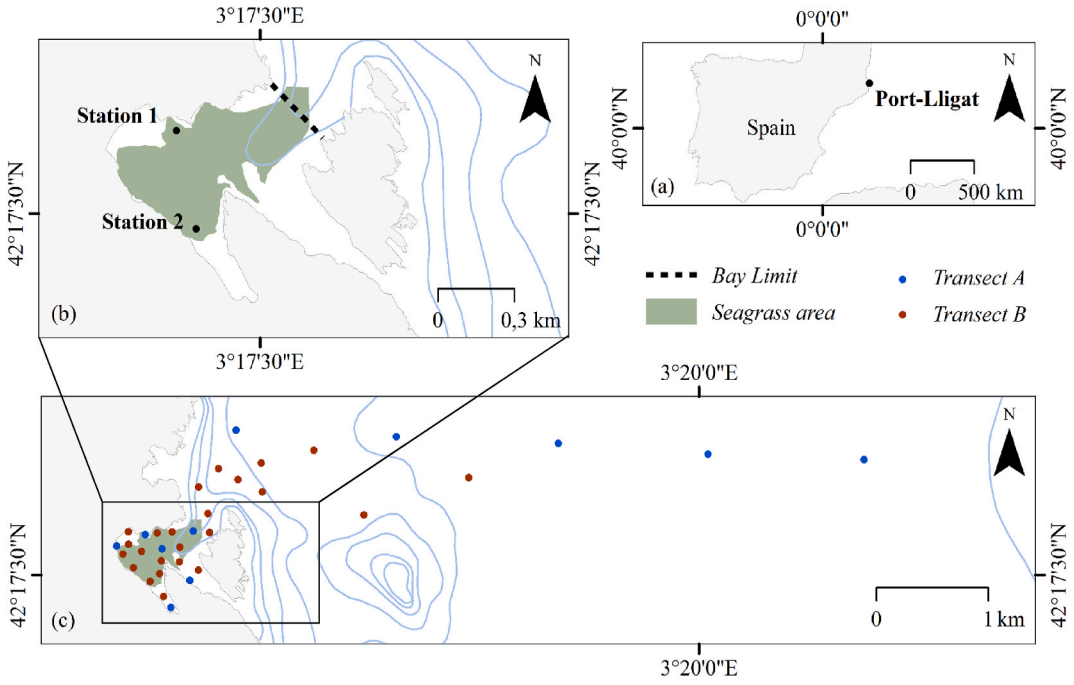

Fig. 1. Study site map. (a) Location of Portlligat bay; (b) Portlligat bay with location of timeseries *Stations 1* and *2*, delineation of bay limit (dotted line) and extent of *Posidonia oceanica* meadows (shaded green) modified from Leiva-Dueñas et al. (2018); (c) Offshore sampling points for *Transect A* (blue) and *Transect B* (red). Bathymetry sourced from GENCAT (2000) displayed as blue contour lines. (For interpretation of the references to colour in this figure legend, the reader is referred to the Web version of this article.)

for estimation of daily GPP and R (Equations (3) and (4)). Sunrise and sunset were defined as 07:00 and 21:00 respectively, determined by insolation data (Hersbach et al., 2018) and online database logs (MapLogs, 2022).

$$\mathrm{GPP} = \Sigma\mathrm{BDO}_{\mathrm{day}} + \left(\left(\Sigma\mathrm{BDO}_{\mathrm{night}}/\mathrm{Hours\ of\ night}\right) \times \mathrm{Hours\ of\ day}\right) \quad (3)$$

$$\mathrm{R} = 24\ \mathrm{x}\ \left(\ \Sigma\mathrm{BDO}_{\mathrm{night}}\ /\ \mathrm{Hours\ of\ night}\ \right) \quad (4)$$

2.3. Bay spatial survey

A spatial survey was conducted on 18th September 2021, between 16:00–17:30. During this time, a 'trace gas analyser' (LI-7810, LI-COR) with precision ± 3.5 ppm was towed throughout the bay. This reports CO_2 in the equilibrator as 'mole fraction in dry air', allowing in-situ pCO_2 to be calculated as a function of temperature, salinity and pressure (Pierrot et al., 2009). Surface water was continuously pumped through an air-water exchanger connected to the gas analyser. Coordinates and corresponding measurements were recorded intermittently (Santos et al., 2012), enabling a map of surface pCO_2 to be interpolated. The pCO_2 values were then used to calculate air-sea gas exchange (Equation (5)). The solubility constant (α) of CO_2 was calculated following methods in Wanninkhof (1992). Atmospheric values for CO_2 were sourced from Lampedusa station records (di Sarra, 2022). Piston velocity (k) was estimated using the parameterisation proposed by Dobashi and Ho (2022) for seagrass systems. Other parameterisations (Ho et al., 2006; Nightingale et al., 2000; Wanninkhof and McGillis, 1999) commonly used for air-sea flux calculations in other Mediterranean seagrass sites (De Carlo et al., 2013; Gazeau et al., 2005) were also estimated (Table 1). Here, we mainly discuss resulting air-sea fluxes relating to the Dobashi and Ho (2022) parameterisation.

$$\mathrm{F} = k \times \alpha \times \left(p\mathrm{co}_{2\mathrm{measured}} - p\mathrm{co}_{2\mathrm{atmosphere}}\right) \quad (5)$$

2.4. Cross-shore transects

Transect surveys were carried out on 12th September 2021, and on 21st – 22nd September 2021. Due to unforeseen differences in weather conditions between transects, results were divided into two separate datasets; *Transect A* (n = 12) and *Transect B* (n = 17). Measurements were taken at ~100 m intervals within the bay and at ~1 km intervals offshore (Fig. 1c). Temperature, pH (NBS scale) and conductivity were measured using probes with precisions of 0.3 °C, 0.02 and 0.06 mS cm^{-1} respectively (PHC101, HACH; CDC401, HACH; TetraCon325, WTW). Samples for TA were stored in 50 mL centrifuge tubes and refrigerated until analysis. TA values were found using the 'Gran approach' with 0.01 mol L^{-1} HCl and a titrator (Metrohm 888 Titrando with Tiamo light) with precision smaller than 5 μmol kg^{-1} (Mos et al., 2021). Drifts and deviations in the acid concentration were corrected using certified reference materials (CRM batch 189), as described by Dickson (2010). Input parameters of TA and pH were then used as inputs for the CO2SYS program to calculate DIC, with a resulting uncertainty of ±16.4 mmol m^{-2} day^{-1} (Lewis et al., 1998; Orr et al., 2018). Carbonate system constants were set to those of Mehrbach et al. (1973) refit by Dickson and Millero (1987).

Radium sampling was also conducted at corresponding transect intervals by collecting 40–60 L of surface water, which were immediately passed through 20 g of manganese fibres at a flow rate of <1 L per minute to quantitatively remove radium from seawater (Moore and Arnold, 1996). Upon return to lab, fibres were thoroughly rinsed with radium free water to remove salt and particles. Fibres were then partially dried and analysed in a Radium Delayed Coincidence Counter system (RaDeCC) to measure activities of ^{223}Ra ($t_{1/2}$ = 11.4 days) and ^{224}Ra ($t_{1/2}$ = 3.66 days). The first round occurred 1 week after sampling and measured initial activities for both isotopes. A second round was conducted after 3 weeks to determine the ^{224}Ra activity supported by ^{228}Th (excess ^{224}Ra) (Moore, 2008).

Outwelling of DIC and TA was estimated following Moore (2000b). This approach treats the shoreline as the only source to the coastal ocean, considers advection as negligible and assumes steady state

inputs. The distribution of ^{223}Ra and ^{224}Ra activity must therefore decrease exponentially offshore due to diffusive mixing and radioactive decay (λ), allowing the calculation of horizontal eddy diffusivity mixing coefficients (*Kh*) (Equation (6)) (Knee et al., 2011; Peterson et al., 2008).

$$Kh = \lambda \,/\, (\,\mathrm{Ln}([\mathrm{Ra}])\mathrm{slope}\,)^2 \tag{6}$$

Outwelling was estimated by multiplying *Kh* with the linear slopes (*m*) of DIC and TA concentrations versus distance from the shoreline (Equation (7)) (Sippo et al., 2019). By multiplying by the depth at the bay limit (Fig. 1b, ~14 m), outwelling can be converted to 'per m shoreline' units.

$$\mathrm{Outwelling} = Kh * m \tag{7}$$

The quantity of DIC which may be lost to the atmosphere (DIC_{excess}) following outwelling was estimated as the difference between the in-situ DIC ($DIC_{in\text{-}situ}$) and the theoretical DIC at atmospheric equilibrium ($DIC_{equilibrium}$) (Equation (8)) (Abril et al., 2000; Maher et al., 2018). $DIC_{equilibrium}$ was obtained using CO2SYS with TA and atmospheric pCO_2 as input parameters. Resulting uncertainty was ±4.2 mmol m^{-2} day^{-1} (Orr et al., 2018).

$$DIC_{excess} = DIC_{in-situ} - DIC_{equilibrium} \tag{8}$$

Isotope activities were also used to derive 'apparent radium age', i.e., the time passed since radium entered the water body. As waters age and mix offshore, both ^{223}Ra and ^{224}Ra will decay at their known respective rates. Thus, by comparing their ratio with an initial ratio, it is possible to derive an apparent age of the water (Equation (9)) (Moore, 2000a; Peterson et al., 2008). The initial ratio was determined as the average ^{223}Ra and ^{224}Ra activity of sediments at five points along the shoreline of the bay. Sediment samples were collected and incubated with seawater for 6 weeks to allow equilibration before analysis.

$$\left[{}^{224}\mathrm{Ra}\,/{}^{223}\mathrm{Ra}\right]_{\mathrm{observed}} = \left[{}^{224}\mathrm{Ra}/{}^{223}\mathrm{Ra}\right]_{\mathrm{initial}} \times \left(e^{-\lambda 224 t}/e^{-\lambda 223 t}\right) \tag{9}$$

Data distributions were assessed using the Shapiro-Wilk test prior to statistical analysis. Following this, differences between the bay and offshore samples were identified using the non-parametric Wilcoxon Rank Sum test. Relationships between variables were assessed using linear regression analysis. Uncertainties for outwelling variables were propagated according to Harvard (2007) and Orr et al. (2018). All calculations were carried out using MATLAB software (MathWorks Inc, R2022b).

3. Results

3.1. Meadow timeseries

Changes in weather and DO were observed throughout the field campaign (Fig. 2). Precipitation generally stayed below 0.5 cm h^{-1}, with the most prominent rain event occurring on September 16th with a peak of 2.5 cm h^{-1}. Wind speeds were on average 4.9 m s^{-1}. Only on September 13th, 14th, 20th and 21st did daily average wind speed exceed 6 m s^{-1}. Sea surface temperature (SST) and irradiance patterns were

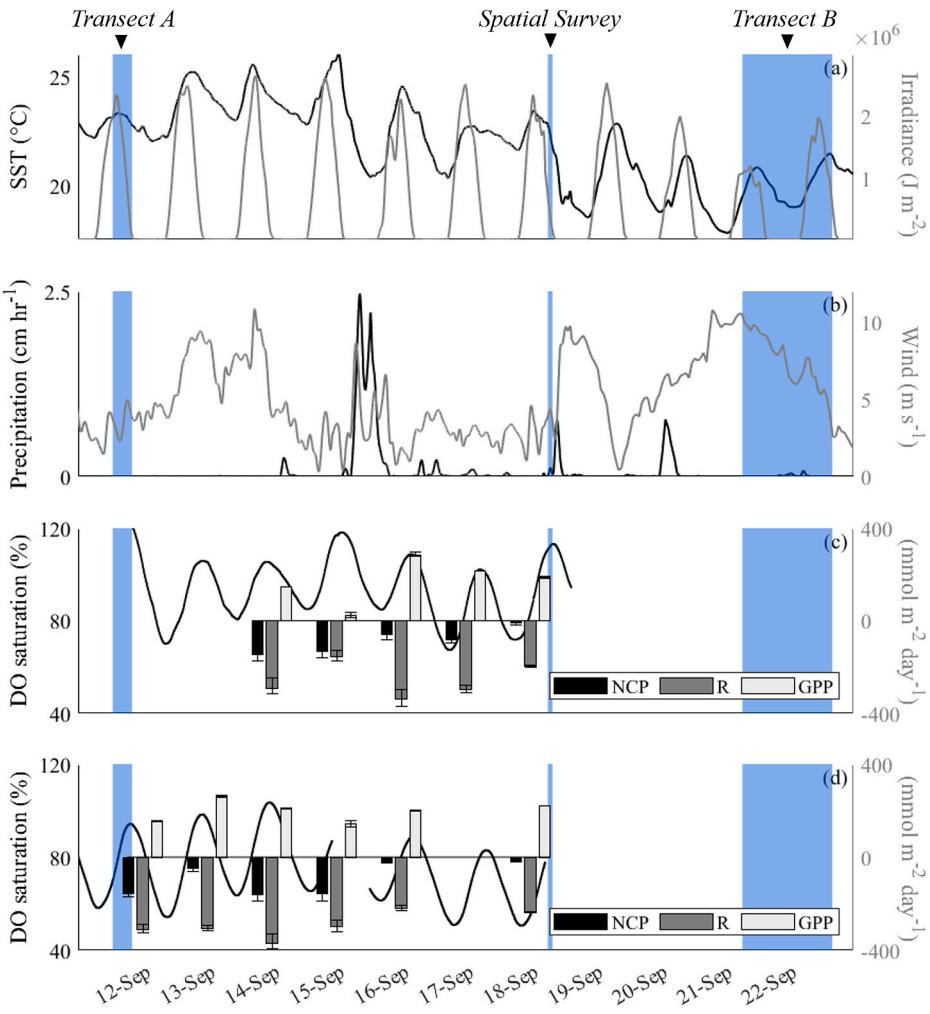

Fig. 2. Timeseries (12th – 22nd September 2022) showing weather parameters sourced from ERA5 reanalysis products (Hersbach et al., 2018) and observations from *Stations 1* and *2*. (a) SST (°C) and irradiance (J m^{-2}); (b) precipitation (cm hr^{-1}) and wind (m s^{-1}); (c & d) dissolved oxygen (DO) saturation percentage (%), daily net community production (NCP) (mmol m^{-2} day^{-1}), respiration (R) (mmol m^{-2} day^{-1}) and gross primary production (GPP) (mmol m^{-2} day^{-1}) for *Stations 1* and *2*. Error bars denote minimum and maximum results from gas parameterisations. Shaded blue areas indicate timings of cross-shore transects *A* and *B*, and bay spatial survey sampling. Colour of axis corresponds to variable display colour. (For interpretation of the references to colour in this figure legend, the reader is referred to the Web version of this article.)

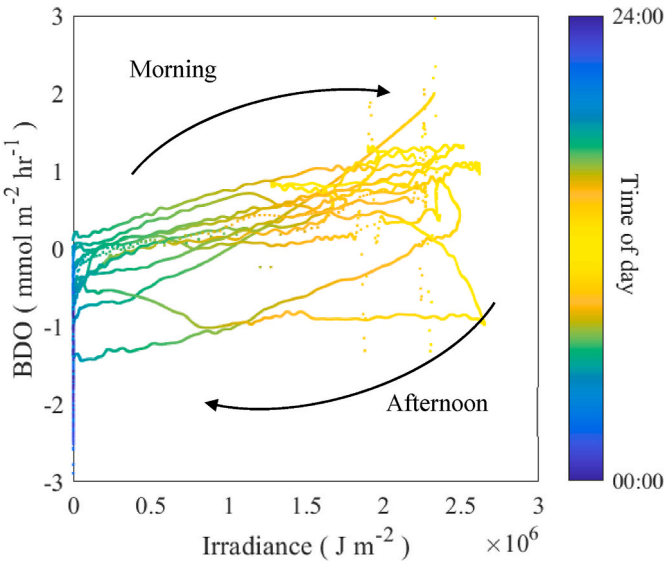

Fig. 3. Scatter plot highlighting hysteresis between irradiance (J m^{-2}) and biological dissolved oxygen change (BDO) (mmol m^{-2} day^{-1}) at *Station 1*. Colour scale represents time of day (hr). Arrows indicate morning and afternoon patterns. Positive BDO represents a release of dissolved oxygen, with negative representing an uptake. (For interpretation of the references to colour in this figure legend, the reader is referred to the Web version of this article.)

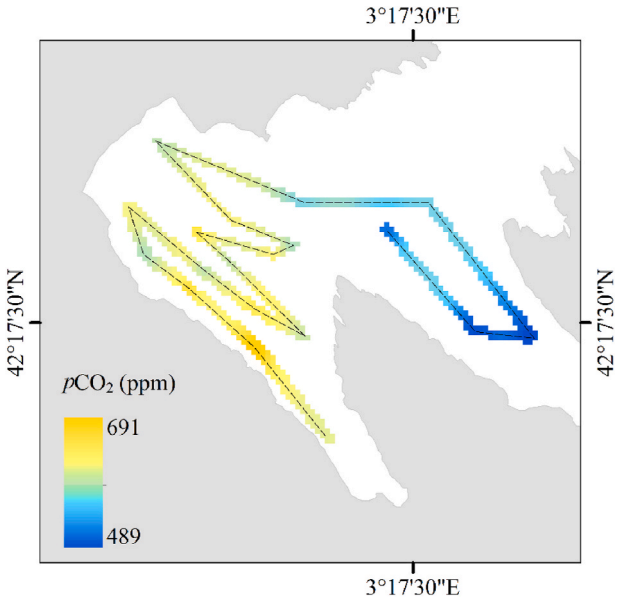

Fig. 4. Spatial distribution of pCO_2 (ppm) in Portlligat bay based on survey measurements taken on 18th September 2021, between 16:00–17:30. Dashed line represents spatial survey track.

consistent with expected diurnal cycles. Irradiance was cumulatively higher in the morning on 10 out of the 13 days, with peaks occurring at ~12:00. $DO_{\%sat}$ also followed a clear diel cycle at both stations (Fig. 2). Values ranged between 51 and 122%, peaking during mid-late afternoon (15:00–18:00). Overall, $DO_{\%sat}$ was higher at *Station 1* (average = 93.6%) than at *Station 2* (average = 75.0%). A hysteresis loop was observed between irradiance and BDO (Fig. 3) demonstrating time lags in DO's response to light. Average BDO's from 00:00–11:59 were −0.1 mmol m^{-2} h^{-1} and −0.04 mmol m^{-2} h^{-1} for *Station 1*, and −0.6 mmol m^{-2} h^{-1} and −0.07 mmol m^{-2} h^{-1} from 12:00–23:59 for *Station 2*.

NCP was negative for all days at both stations, revealing a strong dominance of heterotrophy within the meadow during the early autumn season. NCP averaged −85.8 mmol m^{-2} day^{-1} and −93.2 mmol m^{-2} day^{-1} for *Stations 1 and 2* respectively (Fig. 2c & d). Observations of net heterotrophy also agree with average GPP:R ratios of 0.63 and 0.70, showing the system experienced a greater level of respiration than photosynthesis during the study period.

3.2. Bay spatial survey

pCO_2 was always higher than the atmospheric value of ~411 ppm, therefore generating a concentration gradient from ocean to air. Wind speeds stayed within the range of 3.5–4.3 m s^{-1} during the survey (Fig. 2b). The spatial distribution of pCO_2 reveals particularly high values in the southern inlet (~650 ppm) (Fig. 4). Estimates for piston velocities remained within the same order of magnitude for all parameterisations, with the Dobashi and Ho (2022) parameterisation giving an average value of 2.05 (Table 1). Resulting air-sea CO_2 fluxes within the bay ranged between 1.1 and 4.4 mmol m^{-2} day^{-1}, with a final average flux of 3.0 ± 1.0 mmol m^{-2} day^{-1}.

3.3. Cross-shore transects

The majority of physical parameters showed significant differences between the bay and offshore areas (Table 2). SST values for *Transect A* (mean = 23.9 °C) were markedly higher than those of *Transect B* (mean = 20.8 °C). *Transect B* also showed a 1.4 °C contrast between bay (20.2 °C) and offshore (21.6 °C). Salinities were highest within the bay for both transects (~38.9), reflecting some evaporation in shallow nearshore waters and no freshwater dilution. The overall salinity range was just 1.2, with the average value (38.7) aligning with high values normally expected for the northwest Mediterranean (Álvarez et al., 2014). pH showed clear positive gradients offshore, whilst DIC displayed an opposite distribution (Fig. 5). A clear difference between the bay and offshore waters (Fig. 5d) implied a coastal DIC source, supported by a significant ($p < 0.01$) negative correlation between DIC and distance from shoreline (Fig. 6a). In contrast, the distributional pattern of TA was homogenous (Fig. 5e) with a range of just 71 μmol kg^{-1} and no significant difference ($p > 0.05$) between the bay and offshore (Table 2). Correlations of TA with distance offshore were also non-significant ($p > 0.05$) (Fig. 6), implying no substantial offshore exports of TA. Regression slopes of TA-DIC gave a value 0.03 for both transects, suggesting photosynthesis-respiration processes as a dominant driver of the TA-DIC relationship (Middelburg et al., 2020; Saderne et al., 2019; Zeebe and Wolf-Gladrow, 2001).

Table 1
Piston velocity (k) (cm hr^{-1}) parameterisations and resulting air-sea gas exchange fluxes (mmol m^{-2} day^{-1}). μ_{10m} denotes wind speed at 10 m height above surface level. Flux shown as mean ± standard deviation, with range in brackets.

Parameterisation		k (cm hr^{-1})	Flux (mmol m^{-2} day^{-1})
Nightingale et al. (2000)	$k = 0.23\ (\mu_{10m})^2 + 0.1\ (\mu_{10m})$	4.17 (3.18–4.69)	5.79 ± 1.8 (2.25–8.48)
Wanninkhof and McGillis (1999)	$k = 0.0280\ (\mu_{10m})^3\ (Sc/660)^{-1/2}$	1.72 (1.12–2.06)	2.40 ± 0.8 (0.79–3.46)
Ho et al. (2006)	$k = (0.266 \pm 0.019)\ (\mu_{10m})^2$	4.36 (3.28–4.92)	6.05 ± 1.9 (2.32–8.85)
Dobashi and Ho (2022)	$k = 0.143\ (\mu_{10m})^2$	2.34 (1.76–2.65)	2.98 ± 1.0 (1.07 – 4..44)

Table 2
Mean values (± standard deviation) of all physio-chemical parameters measured within Portlligat bay and offshore as defined by 'bay limit' (Fig. 1b). The statistical significance of differences between the two zones was tested by a Wilcoxon rank sum test. Levels of significance ($p < 0.01$ or $p < 0.05$) are shown.

Parameters	Transect A			Transect B		
	Bay	Offshore	*p* value	Bay	Offshore	*p* value
SST (°C)	24.4 ± 0.4	23.4 ± 0.3	$p < 0.01$	20.2 ± 1	21.6 ± 0.3	$p < 0.01$
Salinity	38.9 ± 0.1	38.7 ± 0.1	$p < 0.01$	38.9 ± 0.2	38.4 ± 0.1	$p < 0.01$
pH	8.2 ± 0.1	8.4 ± 0.1	$p < 0.05$	8.4 ± 0.1	8.5 ± 0.2	$p < 0.05$
DIC (μmol kg^{-1})	2182 ± 82	2032 ± 98	$p > 0.05$	2055 ± 77	1968 ± 150	$p < 0.05$
TA (μmol kg^{-1})	2560 ± 7	2559 ± 6	$p > 0.05$	2563 ± 15	2561 ± 6	$p > 0.05$

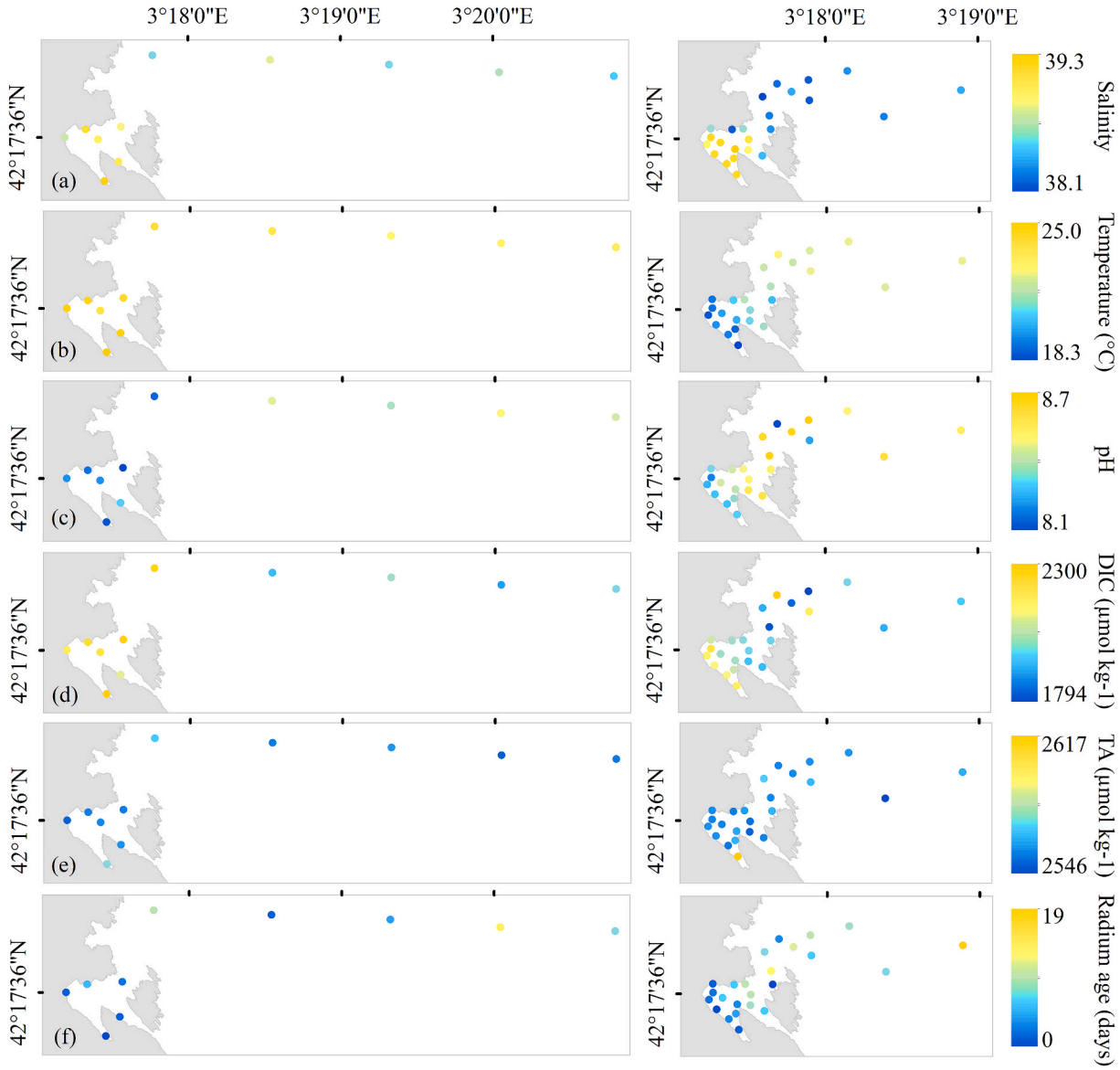

Fig. 5. Spatial distributions of water parameters based on measurements for *Transect A* (left) and *Transect B* (right). (a) Salinity; (b) temperature (°C); (c) pH; (d) dissolved inorganic carbon (DIC) (μmol kg^{-1}); (e) total alkalinity (TA) (μmol kg^{-1}); (f) radium age (days).

^{223}Ra and ^{224}Ra concentration measurements enabled calculation of offshore mixing rates (*Kh*), and radium ages. Both isotopes decreased exponentially with distance from the shoreline, resulting in log linear vs. distance slopes as required for the model (Fig. 7). Mixing rates were similar for both isotopes (0.014 ± 0.0007 and 0.012 ± 0.0004 m^2 s^{-1} for *Transect A*, and 0.013 ± 0.001 and 0.022 ± 0.002 m^2 s^{-1} for *Transect B*) (Table 3). The ratio ^{224}Ra:^{223}Ra decreased in the offshore direction, reflecting the isotopic decay. The apparent radium ages ranged from 0 to 19 days (Fig. 5f) with younger ages found nearshore by the radium source.

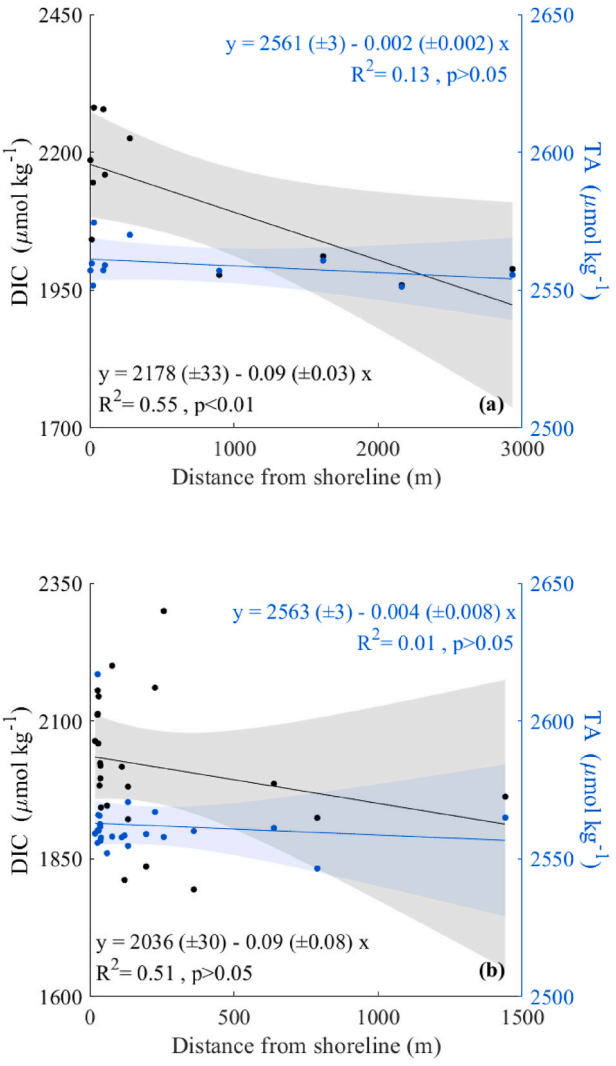

Fig. 6. Dissolved inorganic carbon (DIC) (black) and total alkalinity (TA) (blue) concentrations (μmol kg^{-1}) versus distance from shoreline (m). Slopes (m) are used for outwelling calculations as shown in Equation (7). (a) *Transect A*; (b) *Transect B*. Slope equations are shown with standard errors of coefficients shown in brackets. R^2 and P-value statistics are also displayed. (For interpretation of the references to colour in this figure legend, the reader is referred to the Web version of this article.)

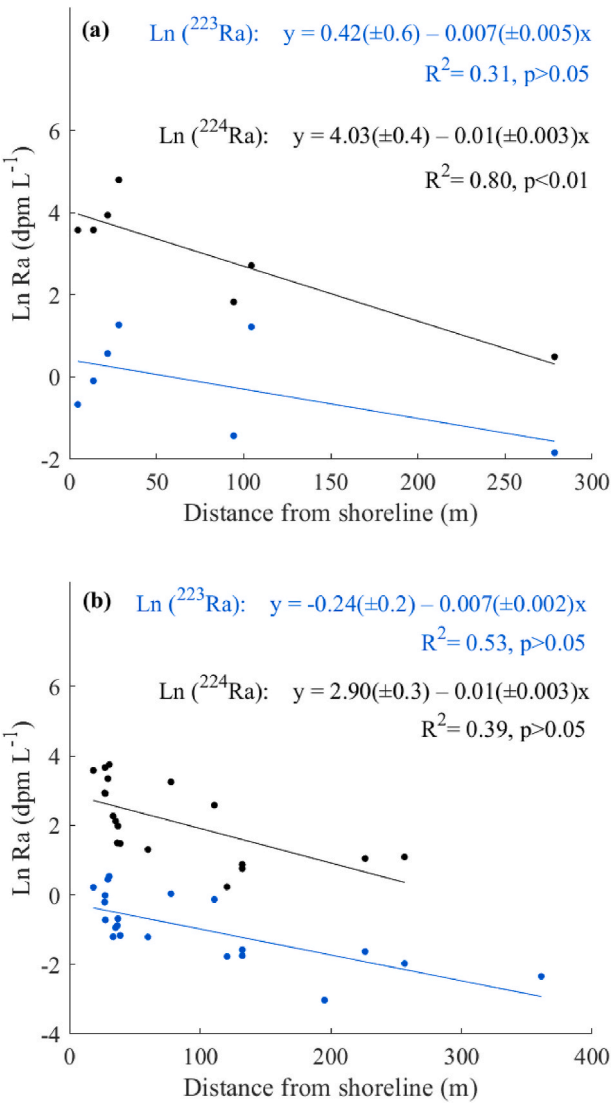

Fig. 7. Distribution of the natural logarithm of ^{223}Ra (blue) and ^{224}Ra (black) surface water activities versus distance from shoreline (m). Slopes are used for calculation of *Kh* in Equation (6). (a) *Transect A*; (b) *Transect B*. Slope equations are shown with standard errors of coefficients shown in brackets. R^2 and P-value statistics are also displayed. (For interpretation of the references to colour in this figure legend, the reader is referred to the Web version of this article.)

Mixing coefficients derived from radium isotopes (*Kh*) were coupled with linear offshore gradients of DIC and TA (*m*) (Table 3) to produce outwelling rates. This resulted in outwelling rates of 98 ± 30 mmol m^{-2} day^{-1} and 130 ± 118 mmol m^{-2} day^{-1} for DIC, and 7 ± 3 mmol m^{-2} day^{-1} and 9 ± 12 mmol m^{-2} day^{-1} for TA for *Transects A and B*, respectively. If the data from the two transects are combined, the average outwelling rates become 114 ± 61 mmol m^{-2} day^{-1} for DIC and 5 ± 6 mmol m^{-2} day^{-1} for TA. Values for DIC outwelling were an order of magnitude greater than those of TA. $DIC_{equilibrium}$ was computed as 3 ± 2 mmol m^{-2} day^{-1} and 22 ± 20 mmol m^{-2} day^{-1} for the *Transects A* and *B* respectively. Pairing these with the measured outwelling rates therefore produced DIC_{excess} of 95 ± 21 mmol m^{-2} day^{-1} and 107 ± 85 mmol m^{-2} day^{-1} for *Transect A* and *B* respectively. This means 96.9% and 82.3% of the total outwelled DIC was likely transferred back to the atmosphere upon reaching the open ocean.

4. Discussion

4.1. Metabolism

Seagrass meadows are complex systems hosting multiple biogeochemical processes (Mateo et al., 2006). During the period of study, the seagrass-dominated bay was controlled by photosynthesis and aerobic respiration. Firstly, clear diel cycles of DO demonstrate a typical photosynthetic response to both light and temperature variations throughout the day (Fig. 2) (Venkiteswaran et al., 2008). This is further supported by the simultaneous production of DIC and lack of TA enrichment. During aerobic respiration, TA experiences minor change, decreasing by just 0.15 mol for each mol of DIC generated (Thomas et al., 2009). The undetectable TA production seen here therefore suggests that aerobic respiration prevailed in the meadow. An oxygenated rhizosphere in surface sediments (Piñeiro-Juncal et al., 2018) and frequent supersaturation of DO in the water column also support this inference. Aerobic processes are highlighted in other pristine Mediterranean *P. oceanica* meadows (Holmer et al., 2004), but Holmer et al.

Table 3
Summary of terms used to estimate horizontal eddy diffusivity mixing coefficients (*Kh*) and outwelling.

	Parameter	Unit	Transect A		Transect B	
			Value	Uncertainty	Value	Uncertainty
Eddy diffusivity	^{223}Ra λ	day^{-1}	0.06		0.06	
	^{224}Ra λ	day^{-1}	0.19		0.19	
	Ln (^{223}Ra) slope	m^{-1}	−0.0071	± 0.00038	−0.0074	± 0.00064
	Ln (^{224}Ra) slope	m^{-1}	−0.0134	± 0.00039	−0.0099	± 0.00069
	Kh 223	$m^2 s^{-1}$	0.014	± 0.00074	0.013	± 0.0011
	Kh 224	$m^2 s^{-1}$	0.012	± 0.00036	0.022	± 0.0015
Offshore linear slope (*m*)	TA	mmol m^{-3} m^{-1}	0.0024	± 0.0021	0.0044	± 0.0082
	DIC	mmol m^{-3} m^{-1}	0.0870	± 0.027	0.0857	± 0.078
Outwelling fluxes	TA	mmol m^{-2} d^{-1}	3	± 2	7	± 12
	DIC	mmol m^{-2} d^{-1}	98	± 30	130	± 118
Outwelling fluxes per m shoreline	TA	mmol m^{-1} d^{-1}	0.2	± 0.2	0.5	± 1
	DIC	mmol m^{-1} d^{-1}	7	± 3	9	± 12

(2003) and Apostolaki et al. (2010b) report anaerobic domination at sites receiving external carbon and nutrient inputs, unlike Portlligat. Lack of TA enrichment, low percentage of carbonates in upper sediment layers (Serrano et al., 2012) and TA-DIC slope values approaching zero (Zeebe and Wolf-Gladrow, 2001) also suggest minimal contribution from carbonate precipitation and dissolution at Portlligat.

Further insights into the photosynthesis-respiration relationship can be drawn by examining the hysteretic response of DO to light (Fig. 3). Effects of daily light cycles go beyond stimulation of photosynthesis and may also act to promote organic carbon mineralisation (Adams et al., 2016; Koopmans et al., 2020; Rheuban, 2013). The increased exudation of organic matter related to photosynthetic activity releases nutrients to the meadow during daylight hours (Adams et al., 2016). This build-up of organic matter and nutrients throughout the day amplifies respiration in the afternoon relative to morning (Rheuban, 2013), explaining the hysteresis pattern. Higher temperatures during early afternoon hours (Fig. 2a) may also amplify aerobic respiration.

Increased respiration explains the negative NCP (mean = −89.5 mmol m^{-2} day^{-1}) and heterotrophic behaviour seen in Portlligat in the early autumn. This may be perceived to contradict the general consensus of seagrass meadows being highly autotrophic over a complete annual cycle (Duarte et al., 2010, 2013; Koopmans et al., 2018). However, similar observations from Gazeau et al. (2005) and Barron and Duarte (2009) also revealed negative NCP in late summer to early autumn. During this time of the year *P. oceanica* canopies in the Mediterranean senesce and net leaf production rates reach minimum values (Serrano et al., 2011) leading to an accumulation of thick seagrass debris deposits (Champenois and Borges, 2012). Not only does this provide readily available substrate for microbial decomposition, but also results in a loss of photosynthetic material from the already slow growing *P. oceanica* (Barron and Duarte, 2009). Environmental conditions may also exacerbate the GPP:R ratio as the late summer – early autumn period brings reduced irradiance that further hampers photosynthesis, as well as rain that can enhance terrestrial nutrient run-off (Alcoverro et al., 1995). Oxygenated conditions in seagrass rhizospheres (Borum et al., 2006; Marbà et al., 2010; Piñeiro-Juncal et al., 2020), also promote the more efficient aerobic respiration as opposed to anaerobic processes. As a result, heterotrophy and aerobic mineralisation in Portlligat released DIC to the water column during early autumn.

4.2. Air-sea CO_2 flux

The insight from DO observations in Portlligat is consistent with both the magnitude and spatial distribution of pCO_2. Overall, sea surface pCO_2 exceeded atmospheric partial pressures throughout the entire bay. The source of this CO_2 is likely seagrass heterotrophy and aerobic mineralisation. Furthermore, higher pCO_2 values were found in the southern inlet where meadow coverage is sparse and less healthy (Fig. 1b). This is likely explained by reduced photosynthetic activity and increased decomposition (Champenois and Borges, 2021; Liu et al., 2017; Roca et al., 2022), as well as geomorphology of the area which promotes accumulation of debris and longer residence times. Outgassing CO_2 fluxes (3.0 ± 1.0 mmol m^{-2} day^{-1}) are of similar magnitude to those seen in other Mediterranean *P. oceanica* meadows at the same time of year. Frankignoulle (1988) reported values of 6.2 mmol m^{-2} day^{-1} for August and 10.8 mmol m^{-2} day^{-1} in October. Given the similar sampling season and low winds (<3 m s^{-1}), the slight difference between values established here and those of Frankignoulle (1988) are attributed to stronger air-sea gradients and chamber techniques which produced two-fold larger piston velocities (Matthews et al., 2003). Gazeau et al. (2005) also reported fluxes within the same range, suggesting source behaviour throughout summer seasons, with net ecosystem production being most negative in late summer – early autumn after high organic matter production. In comparison, Champenois and Borges (2021) suggested a net annual air-sea flux of –1.9 mmol m^{-2} day^{-1} for another seagrass populated Mediterranean bay.

There are potential uncertainties in the CO_2 emission estimates presented. For example, spatial and temporal heterogeneities in wind speed and temperature drive uncertainty. Van Dam et al. (2021a) attributed 23% of diurnal variability in CO_2 flux above a seagrass meadow to the effect of changing water temperatures on gas solubility. Zhang and Fischer (2014) also highlighted the impact of biological influence on daily CO_2 fluctuations. The spatial survey in Portlligat was conducted in the late afternoon, 2 hours post peak temperatures and corresponding with the period of greatest respiration (Figs. 2 and 4). Furthermore, the spatial survey for gas exchange was performed when wind speed values were below the mean (Fig. 2b). Piston velocity parameterisations present another source of uncertainty to flux calculations. The parameterisation employed here is applicable for coastal seagrass ecosystems, and developed in a bay with similar characteristics to Portlligat during the study period (e.g. limited wind fetch, relatively shallow, minimal tides, low wind speeds) (Dobashi and Ho, 2022).

4.3. Outwelling of DIC and TA

This study provides one of the first estimates for DIC outwelling in seagrass meadows. Lateral transport of DIC originated from within the bay. As implied from the DO timeseries and the pCO_2 spatial survey, the most plausible source of DIC at this site is heterotrophic behaviour of the *P. oceanica* meadow during early autumn. Although comparisons to other DIC observations are limited, evaluation against DOC outwelling can be made. Barron and Duarte (2009) estimated DOC outwelling from the *P. oceanica* at Magalluf bay to be 12.2 ± 4.3 mmol m^{-2} day^{-1} for the month of September. Similarly, Apostolaki et al. (2010a) provided estimates of 7.2 ± 2.6 mmol m^{-2} day^{-1} in August and 12.6 ± 4.5 mmol m^{-2} day^{-1} in October for a *P. oceanica* meadow in Greece. The magnitude of DIC outwelling calculated here (114 ± 61 mmol m^{-2} day^{-1}) is an order of magnitude larger than those of the previously recognised DOC.

Hence, DIC export seems to be a significant component of the seagrass carbon budget, as also observed in mangrove and saltmarsh ecosystems (Maher et al., 2018; Yau et al., 2022).

Once DIC reaches the ocean, it can follow two potential paths — emission to the atmosphere as CO_2 or sequestration in the oceanic pool (Santos et al., 2021). At Portlligat, DIC outwelling (114 ± 61 mmol m^{-2} day^{-1}) was accompanied by a minor export of TA (5 ± 6 mmol m^{-2} day^{-1}). Without a source of TA, CO_2 derived from net heterotrophy will not be converted to carbonate alkalinity (Raymond et al., 2000; Santos et al., 2019). In addition, $DIC_{equilibrium's}$ were just 3% and 18% of total outwelled DIC for *Transects A* and *B* respectively. Hence, the majority of DIC was potentially returned to the atmosphere and represents an overlooked carbon emission pathway from the seagrass system during early autumn.

Although not all components of the carbon budget were quantified in this study, a preliminary assessment can be made. The local long-term carbon burial rate in sediments at Portlligat is 17 mmol m^{-2} day^{-1} (Serrano et al., 2012). If just considering above-meadow outgassing (3.0 ± 1.0 mmol m^{-2} day^{-1}), the seagrass meadow would be perceived as a CO_2 sink. However, average DIC outwelling was >20-times larger than CO_2 lost via outgassing within the bay. Combining the portion of DIC that is outgassed following export (average DIC_{excess} = 101 ± 44 mmol m^{-2} day^{-1}) with above-meadow emissions (3.0 ± 1.0 mmol m^{-2} day^{-1}) gives a total loss of 104 ± 22 mmol m^{-2} day^{-1}. Hence, carbon emissions following offshore outwelling potentially exceed long term sequestration in local soils by > 500% during the study period. Further investigations encompassing all seasons of the year are required to close the overall carbon budget at Portlligat. This is also relevant when evaluating the contribution of NCP to outwelling. The fact that total DIC outwelling (114 ± 61 mmol m^{-2} day^{-1}) exceeded NCP (mean = −89.5 mmol m^{-2} day^{-1}) can be explained by the different resolutions and timescales of processes captured by measurements. *P. oceanica* produces largest negative NCP in August (Gazeau et al., 2005). Estimations for outwelling may depict conditions from these prior weeks, explaining the disparity.

The use of radium isotopes in this study represents an example of their application to outwelling investigations in seagrass meadows. Activities of both ^{223}Ra and ^{224}Ra displayed an exponential decrease with distance offshore, confirming the shoreline as the major source (Moore, 2000b). Strong stratification during late summer – early autumn (Bégovic and Copin-Montégut, 2002) and coarse nature of sediments (Serrano et al., 2012) further confirms the lack of additional inputs from offshore sediment diffusion or suspended particles (Dulaiova and Burnett, 2008; Hougham and Moran, 2007; Tait et al., 2013). The linear fit of the log distributions demonstrates control via eddy diffusivity rather than horizontal advection (Burnett et al., 2008), inferred also by limited tidal action at the site (Schmidt et al., 2011). Similarities between *Kh*'s of both ^{223}Ra and ^{224}Ra imply a system approaching steady state on timescales of weeks (Charette et al., 2007; Yadav and Jha, 2019). The slight discrepancy between *Kh*'s calculated for *Transect B* could be associated with changing wind conditions influencing mixing processes on the timescale of ^{224}Ra decay (Dulaiova and Burnett, 2008; Moore and de Oliveira, 2008).

5. Conclusion

This study presents some of the first estimates for DIC and TA outwelling from a seagrass meadow. The lateral exports of DIC were larger than previously estimated for DOC, and >20-times greater than above-meadow CO_2 outgassing. DIC production was fuelled by seagrass heterotrophy and aerobic metabolism. Uncoupled TA generation and export suggested that the majority of outwelled DIC was recycled back to the atmosphere as CO_2. DIC outwelling at this site therefore acted as a loss pathway from the system during early autumn, potentially opposing some of the 'blue carbon' sequestration within sediments. Further work quantifying DIC and alkalinity outwelling in seagrass meadows is vital for determining its annual contribution to seagrass carbon budgets, together with DOC and POC fluxes. Radium isotopes could be used to resolve mixing rates and offshore transport.

CRediT authorship contribution statement

Claudia Majtényi-Hill: Visualization, Investigation, Conceptualization, Writing – original draft, Writing – review & editing. **Gloria Reithmaier:** Supervision, Investigation, Writing – review & editing. **Yvonne Y.Y. Yau:** Investigation, Writing – review & editing. **Oscar Serrano:** Investigation, Funding acquisition, Writing – review & editing. **Nerea Piñeiro-Juncal:** Investigation, Writing – review & editing. **Isaac R. Santos:** Supervision, Investigation, Funding acquisition, Conceptualization, Writing – review & editing.

Declaration of competing interest

The authors declare that they have no known competing financial interests or personal relationships that could have appeared to influence the work reported in this paper

Data availability

Data will be made available on request.

Acknowledgements

This project was funded by the Swedish Research Council (2020–00457). OS was supported by I + D + i projects RYC2019-027073-I and PIE HOLOCENO 20213AT014 funded by MCIN/AEI/10.13039/501100011033 and FEDER. N. P-J. was supported by the Programme for Requalification of the Spanish University System 2021–2023 (Ministerio de Universidades), modality Margarita Salas, and financial support to CESAM (UIDB/50017/2020, UIDP/50017/2020, and LA/P/0094/2020; FCT/MCTES).

References

Abril, G., Etcheber, H., Borges, A.V., Frankignoulle, M., 2000. Excess atmospheric carbon dioxide transported by rivers into the Scheldt estuary. Comptes Rendus Acad. Sci. - Ser. IIA Earth Planet. Sci. 330, 761–768.

Adams, M.P., Ferguson, A.J.P., Maxwell, P.S., Lawson, B.A.J., Samper-Villarreal, J., O'Brien, K.R., 2016. Light history-dependent respiration explains the hysteresis in the daily ecosystem metabolism of seagrass. Hydrobiologia 766, 75–88.

Alcoverro, T., Duarte, C.M., Romero, J., 1995. Annual growth dynamics of Posidonia oceanica: contribution of large-scale versus local factors to seasonality. Mar. Ecol. Prog. Ser. 120, 203–210.

Álvarez, M., Sanleón-bartolomé, H., Tanhua, T., Mintrop, L., Luchetta, A., Cantoni, C., Schroeder, K., Civitarese, G., 2014. The CO_2 system in the Mediterranean Sea: a basin wide perspective. Ocean Sci. 10, 69–92.

Apostolaki, E., Holmer, M., Marba, N., Karakassis, I., 2010a. Degrading seagrass (Posidonia oceanica) ecosystems: a source of dissolved matter in the Mediterranean. Hydrobiologia 649, 13–23.

Apostolaki, E., Holmer, M., Marba, N., Karakassis, I., 2010b. Metabolic imbalance in coastal vegetated (Posidonia oceanica) and unvegetated benthic ecosystems. Ecosystems 13, 459–471.

Barron, C., Apostolaki, E.T., Duarte, C.M., 2014. Dissolved organic carbon fluxes by seagrass meadows and macroalgal beds. Front. Mar. Sci. 1.

Barron, C., Duarte, C., 2009. Dissolved organic matter release in Posidonia oceanica meadow. Marine Ecology-progress Series - MAR ECOL-PROGR SER 374, 75–84.

Barron, C., Duarte, C.M., Frankignoulle, M., Borges, A.V., 2006. Organic carbon metabolism and carbonate dynamics in a Mediterranean seagrass (Posidonia oceanica), meadow. Estuar. Coast 29, 417–426.

Begovic, M., Copin-Montegut, C., 2002. Processes controlling annual variations in the partial pressure of CO_2 in surface waters of the central northwestern Mediterranean Sea (Dyfamed site). Deep Sea Res. Part II Top. Stud. Oceanogr. 49, 2031–2047.

Borum, J., Sand-Jensen, K., Binzer, T., Pedersen, O., Maria, T., Greve, 2006. Oxygen movement in seagrasses. In: Larkum, A.W.D., Orth, R.J., Duarte, C.M. (Eds.), Seagrasses: Biology, Ecology and Conservation. Springer Netherlands, Dordrecht, pp. 255–270.

Burnett, W.C., Peterson, R., Moore, W.S., de Oliveira, J., 2008. Radon and radium isotopes as tracers of submarine groundwater discharge - results from the Ubatuba, Brazil SGD assessment intercomparison. Estuarine. Coastal and Shelf Science 76, 501–511.

Burt, D.J., Frob, F., Ilyina, T., 2021. The sensitivity of the marine carbonate system to regional ocean alkalinity enhancement. Frontiers in Climate 3.
Cabral, A., Dittmar, T., Call, M., Scholten, J., de Rezende, C.E., Asp, N., Gledhill, M., Seidel, M., Santos, I.R., 2021. Carbon and alkalinity outwelling across the groundwater-creek-shelf continuum off Amazonian mangroves. Limnology and Oceanography Letters 6, 369–378.
Champenois, W., Borges, A., 2012. Seasonal and inter-annual variation of community metabolism rates of a Posidonia oceanica seagrass meadow. Limnol. Oceanogr. 57, 347–361.
Champenois, W., Borges, A.V., 2021. Net community metabolism of a Posidonia oceanica meadow. Limnol. Oceanogr. 66, 2126–2140.
Charette, M.A., Gonneea, M.E., Morris, P.J., Statham, P.J., Fones, G.R., Planquette, H., Salter, I., Garabato, A.N., 2007. Radium isotopes as tracers of iron sources fueling a Southern Ocean phytoplankton bloom. Deep-sea Research Part Ii-topical Studies in Oceanography 54, 1989–1998.
Chou, W.-C., Chu, H.-C., Chen, Y.-H., Syu, R.-W., Hung, C.-C., Soong, K., 2018. Short-term variability of carbon chemistry in two contrasting seagrass meadows at Dongsha Island: implications for pH buffering and CO2 sequestration. Estuar. Coast Shelf Sci. 210, 36–44.
Chou, W.-C., Fan, L.-F., Yang, C.-C., Chen, Y.-H., Hung, C.-C., Huang, W.-J., Shih, Y.-Y., Soong, K., Tseng, H.-C., Gong, G.-C., Chen, H.-Y., Su, C.-K., 2021. A unique diel pattern in carbonate chemistry in the seagrass meadows of dongsha island: the enhancement of metabolic carbonate dissolution in a semienclosed lagoon. Front. Mar. Sci. 8.
Cole, J.J., Hararuk, O., Solomon, C.T., 2021. Chapter 7 - the carbon cycle: with a brief introduction to global biogeochemistry. In: Weathers, K.C., Strayer, D.L., Likens, G.E. (Eds.), Fundamentals of Ecosystem Science, second ed. Academic Press, pp. 131–160.
De Carlo, E., Laure, M., Passafiume, O., Drupp, P., Gattuso, J.-P., 2013. Carbonate chemistry and air-sea CO_2 flux in a NW Mediterranean bay over a four-year period: 2007-2011. Aquat. Geochem. 19, 399–442.
di Sarra, A.P.S., 2022. ICOS ATC NRT CO_2 Growing Time Series, Lampedusa (8.0 M). Atmosphere Thematic Centre, p. 2021, 02-01–2022-03-09.
Dickson, A.G., 2010. Standards for ocean measurements Oceanography 23, 34–47.
Dickson, A.G., Millero, F.J., 1987. A comparison of the equilibrium constants for the dissociation of carbonic acid in seawater media. Deep Sea Research Part A. Oceanographic Research Papers 34, 1733–1743.
Dobashi, R., Ho, D.T., 2022. Air-sea gas exchange in a seagrass ecosystem. EGUsphere 2022, 1–21.
Duarte, C., Krause-Jensen, D., 2017. Export from seagrass meadows contributes to marine carbon sequestration. Front. Mar. Sci. 4.
Duarte, C., Marba, N., Gacia, E., Fourqurean, J., Beggins, J., Barron, C., Apostolaki, E., 2010. Seagrass community metabolism: assessing the carbon sink capacity of seagrass meadows. Global Biogeochem. Cycles 24.
Duarte, C.M., Kennedy, H., Marbà, N., Hendriks, I., 2013. Assessing the capacity of seagrass meadows for carbon burial: current limitations and future strategies. Ocean Coast Manag. 83, 32–38.
Dulaiova, H., Burnett, W.C., 2008. Evaluation of the flushing rates of Apalachicola Bay, Florida via natural geochemical tracers. Mar. Chem. 109, 395–408.
Dunic, J.C., Brown, C.J., Connolly, R.M., Turschwell, M.P., Côté, I.M., 2021. Long-term declines and recovery of meadow area across the world's seagrass bioregions. Global Change Biol. 27, 4096–4109.
ECMWF, 2022. Water Level Change Indicators for the European Coast from 1977 to 2100 Derived from Climate Projections. EU Copernicus Climate Change Service. Climate Data Store (CDS).
Fourqurean, J.W., Duarte, C.M., Kennedy, H., Marbà, N., Holmer, M., Mateo, M.A., Apostolaki, E.T., Kendrick, G.A., Krause-Jensen, D., McGlathery, K.J., Serrano, O., 2012. Seagrass ecosystems as a globally significant carbon stock. Nat. Geosci. 5, 505–509.
Frankignoulle, M., 1988. Field measurements of air-sea CO_2 exchange. Limnol. Oceanogr. 33, 313–322.
Ganguly, D., Singh, G., Ramachandran, P., Selvam, A.P., Banerjee, K., Ramachandran, R., 2017. Seagrass metabolism and carbon dynamics in a tropical coastal embayment. Ambio 46, 667–679.
Gazeau, F., Duarte, C.M., Gattuso, J.P., Barron, C., Navarro, N., Ruiz, S., Prairie, Y.T., Calleja, M., Delille, B., Frankignoulle, M., Borges, A.V., 2005. Whole-system metabolism and CO_2 fluxes in a mediterranean bay dominated by seagrass beds (palma bay, NW mediterranean). Biogeosciences 2, 43–60.
Gencat, 2000. Batimetría carta nautica IHM (1976-1996). In: Sostenible, S.-P.-D.G. (Ed.), Departamento de Acción Climática, Alimentación y Agenda Rural (Generalitat de Catalunya).
Harvard, 2007. A Summary of Error Propagation. Harvard University Press, Cambridge, MA.
Hersbach, H., Bell, B., Berrisford, P., Biavati, G., Horanyi, A., Munoz Sabater, J., Nicolas, J., Peubey, C., Radu, R., Rozum, I., Schepers, D., Simmons, A., Soci, C., Dee, D., Thepaut, J.-N., 2018. ERA5 hourly data on single levels from 1979 to present. Copernicus Climate Change Service (C3S), Climate Data Store (CDS). https://doi.org/10.24381/cds.adbb2d47 (Accessed on < 04-Jan-2022 >).
Ho, D.T., Law, C.S., Smith, M.J., Schlosser, P., Harvey, M., Hill, P., 2006. Measurements of air-sea gas exchange at high wind speeds in the Southern Ocean: implications for global parameterizations Geophys. Geophys. Res. Lett. 33.
Holmer, M., Duarte, C., Boschker, H., Barron, C., 2004. Carbon cycling and bacterial carbon sources in pristine and impacted Mediterranean seagrass sediments. Aquatic Microbial Ecology - AQUAT MICROB ECOL 36, 227–237.
Holmer, M., Duarte, C.M., Marbá, N., 2003. Sulfur cycling and seagrass (Posidonia oceanica) status in carbonate sediments. Biogeochemistry 66, 223–239.
Hougham, A.L., Moran, S.B., 2007. Water mass ages of coastal ponds estimated using ^{223}Ra and ^{224}Ra as tracers. Mar. Chem. 105, 194–207.
Hu, X., Cai, W.-J., 2011. An assessment of ocean margin anaerobic processes on oceanic alkalinity budget. Global Biogeochem. Cycles 25.
Ismail, R.O., 2021. Drivers of carbon sink function in tropical seagrass beds : influence of carbon import, plant composition, seascape configuration and human activities (PhD dissertation). In: Department of Ecology, E.a.P.S. Stockholm University.
Knee, K., Garcia Solsona, E., Garcia-Orellana, J., Boehm, A., 2011. Using radium isotopes to characterize water ages and coastal mixing rates: a sensitivity analysis: radium sensitivity analysis. Limnol Oceanogr. Methods 9.
Koopmans, D., Holtappels, M., Chennu, A., Weber, M., de Beer, D., 2018. The response of seagrass (Posidonia oceanica) meadow metabolism to CO_2 levels and hydrodynamic exchange determined with aquatic eddy covariance. Biogeosci. Discuss. 1–23, 2018.
Koopmans, D., Holtappels, M., Chennu, A., Weber, M., de Beer, D., 2020. High net primary production of Mediterranean seagrass (Posidonia oceanica) meadows determined with aquatic eddy covariance. Front. Mar. Sci. 7.
Leiva-Duenas, C., Lopez-Merino, L., Serrano, O., Martinez Cortizas, A., Mateo, M.A., 2018. Millennial-scale trends and controls in Posidonia oceanica (L. Delile) ecosystem productivity. Global Planet. Change 169, 92–104.
Lewis, E., Wallace, D., Allison, L.J., 1998. Program Developed for CO_2 System Calculations, United States, p. 40. Medium: ED; Size:
Liu, S., Jiang, Z., Deng, Y., Wu, Y., Zhao, C., Zhang, J., Shen, Y., Huang, X., 2017. Effects of seagrass leaf litter decomposition on sediment organic carbon composition and the key transformation processes. Sci. China Earth Sci. 60, 2108–2117.
Lo Iacono, C., Mateo, M.A., Gracia, E., Guasch, L., Carbonell, R., Serrano, L., Serrano, O., Danobeitia, J., 2008. Very high-resolution seismo-acoustic imaging of seagrass meadows (Mediterranean Sea): implications for carbon sink estimates. Geophys. Res. Lett. 35.
Macreadie, P.I., Anton, A., Raven, J.A., Beaumont, N., Connolly, R.M., Friess, D.A., Kelleway, J.J., Kennedy, H., Kuwae, T., Lavery, P.S., Lovelock, C.E., Smale, D.A., Apostolaki, E.T., Atwood, T.B., Baldock, J., Bianchi, T.S., Chmura, G.L., Eyre, B.D., Fourqurean, J.W., Hall-Spencer, J.M., Huxham, M., Hendriks, I.E., Krause-Jensen, D., Laffoley, D., Luisetti, T., Marba, N., Masque, P., McGlathery, K.J., Megonigal, J.P., Murdiyarso, D., Russell, B.D., Santos, R., Serrano, O., Silliman, B.R., Watanabe, K., Duarte, C.M., 2019. The future of Blue Carbon science. Nat. Commun. 10, 3998.
Macreadie, P.I., Nielsen, D.A., Kelleway, J.J., Atwood, T.B., Seymour, J.R., Petrou, K., Connolly, R.M., Thomson, A.C., Trevathan-Tackett, S.M., Ralph, P.J., 2017. Can we manage coastal ecosystems to sequester more blue carbon? Front. Ecol. Environ. 15, 206–213.
Maher, D.T., Call, M., Santos, I.R., Sanders, C.J., 2018. Beyond burial: lateral exchange is a significant atmospheric carbon sink in mangrove forests. Biol. Lett. 14.
MapLogs, 2022. Sunrise Sunset Times Lookup.
Marba, N., Duarte, C.M., Terrados, J., Halun, Z., Gacia, E., Fortes, M.D., 2010. Effects of seagrass rhizospheres on sediment redox conditions in SE asian coastal ecosystems. Estuar. Coast 33, 107–117.
Mateo, M., Cebrian, J., Dunton, K., Mutchler, T., Larkum, A., Orth, R., Duarte, C., 2006. Carbon Flux in Seagrass Ecosystems, pp. 159–192.
Mateo, M.A., Romero, J., 1997. Detritus dynamics in the seagrass Posidonia oceanica: elements for an ecosystem carbon and nutrient budget. Mar. Ecol. Prog. Ser. 151, 43–53.
Matthews, C.J.D., St Louis, V.L., Hesslein, R.H., 2003. Comparison of three techniques used to measure diffusive gas exchange from sheltered aquatic surfaces. Environ. Sci. Technol. 37, 772–780.
Maxwell, P.S., Eklof, J.S., van Katwijk, M.M., O'Brien, K.R., de la Torre-Castro, M., Bostrom, C., Bouma, T.J., Krause-Jensen, D., Unsworth, R.K.F., van Tussenbroek, B. I., van der Heide, T., 2017. The fundamental role of ecological feedback mechanisms for the adaptive management of seagrass ecosystems – a review. Biol. Rev. 92, 1521–1538.
Mcleod, E., Chmura, G.L., Bouillon, S., Salm, R., Bjork, M., Duarte, C.M., Lovelock, C.E., Schlesinger, W.H., Silliman, B.R., 2011. A blueprint for blue carbon: toward an improved understanding of the role of vegetated coastal habitats in sequestering CO_2. Front. Ecol. Environ. 9, 552–560.
Mehrbach, C., Culberson, C.H., Hawley, J.E., Pytkowicx, R.M., 1973. Measurement of the apparent dissociation constants of carbonic acid in seawater at atmospheric pressure. Limnol. Oceanogr. 18, 897–907.
Middelburg, J.J., Soetaert, K., Hagens, M., 2020. Ocean alkalinity, buffering and biogeochemical processes. Rev. Geophys. 58, e2019RG000681.
Millero, F.J., 2007. The marine inorganic carbon cycle. Chem. Rev. 107, 308–341.
Moore, W.S., 2000a. Ages of continental shelf waters determined from ^{223}Ra and ^{224}Ra. J. Geophys. Res.: Oceans 105, 22117–22122.
Moore, W.S., 2000b. Determining coastal mixing rates using radium isotopes. Continent. Shelf Res. 20, 1993–2007.
Moore, W.S., 2008. Fifteen years experience in measuring ^{224}Ra and ^{223}Ra by delayed-coincidence counting. Mar. Chem. 109, 188–197.
Moore, W.S., Arnold, R., 1996. Measurement of ^{223}Ra and ^{224}Ra in coastal waters using a delayed coincidence counter. J. Geophys. Res.: Oceans 101, 1321–1329.
Moore, W.S., de Oliveira, J., 2008. Determination of residence time and mixing processes of the Ubatuba, Brazil, inner shelf waters using natural Ra isotopes. Estuar. Coast Shelf Sci. 76, 512–521.
Mos, B., Holloway, C., Kelaher, B.P., Santos, I.R., Dworjanyn, S.A., 2021. Alkalinity of diverse water samples can be altered by mercury preservation and borosilicate vial storage. Sci. Rep. 11, 9961.
Needoba, J.A., Peterson, T.D., Johnson, K.S., 2012. Method for the quantification of aquatic primary production and net ecosystem metabolism using in situ dissolved

oxygen sensors. In: Tiquia-Arashiro, S.M. (Ed.), Molecular Biological Technologies for Ocean Sensing. Humana Press, Totowa, NJ, pp. 73–101.
Nelleman, C., Corcoran, E., Duarte, C.M., Valdes, L., DeYoung, C., Fonseca, L., Grimsditch, G., 2008. Blue Carbon: the Role of Healthy Oceans in Binding Carbon. UNEP/FAO/UNESCO/IUCN/CSIC.
Nightingale, P.D., Malin, G., Law, C.S., Watson, A.J., Liss, P.S., Liddicoat, M.I., Boutin, J., Upstill-Goddard, R.C., 2000. In situ evaluation of air-sea gas exchange parameterizations using novel conservative and volatile tracers. Global Biogeochem. Cycles 14, 373–387.
Odum, H.T., 1956. Primary production in flowing waters. Limnol. Oceanogr. 1, 102–117.
Orr, J.C., Epitalon, J.-M., Dickson, A.G., Gattuso, J.-P., 2018. Routine uncertainty propagation for the marine carbon dioxide system. Mar. Chem. 207, 84–107.
Peterson, R., Burnett, W., Taniguchi, M., Chen, J., Misra, S., 2008. Determination of transport rates in the Yellow River–Bohai Sea mixing zone via natural geochemical tracers. Continental Shelf Research - CONT SHELF RES 28, 2700–2707.
Pierrot, D., Neill, C., Sullivan, K., Castle, R., Wanninkhof, R., Luger, H., Johannessen, T., Olsen, A., Feely, R.A., Cosca, C.E., 2009. Recommendations for autonomous underway pCO2 measuring systems and data-reduction routines. Deep Sea Res. Part II Top. Stud. Oceanogr. 56, 512–522.
Pimenta, A.R., Grear, J.S., 2018. Guidelines for Measuring Changes in Seawater pH and Associated Carbonate Chemistry in Coastal Environments of the Eastern United States. Environment Protection Agency, Narragansett, RI, U.S, p. 59pp. EPA/600/R-17/483.
Pineiro-Juncal, N., Leiva-Duenas, C., Serrano, O., Mateo, M.A., Martinez-Cortizas, A., 2020. Pedogenic processes in a Posidonia oceanica mat. Soil Systems 4, 18.
Pineiro-Juncal, N., Mateo, M., Holmer, M., Martinez-Cortizas, A., 2018. Potential microbial functional activity along a Posidonia oceanica soil profile. Aquat. Microb. Ecol. 81, 189–200.
Raymond, P., Bauer, J., Cole, J., 2000. Atmospheric CO_2 evasion, dissolved inorganic carbon production, and net heterotrophy in the York River Estuary. Limnol. Oceanogr. 45, 1707–1717.
Rheuban, J.E., 2013. Oxygen Metabolism in Restored Eelgrass (Zostera Marina L.) Meadows Measured by Eddy Correlation. M.S. Thesis). University of Virginia, Charlottesville, VA.
Roca, G., Palacios, J., Ruiz-Halpern, S., Marbà, N., 2022. Experimental carbon emissions from degraded mediterranean seagrass (Posidonia oceanica) meadows under current and future summer temperatures. J. Geophys. Res.: Biogeosciences 127, e2022JG006946.
Ruiz Fernandez, J.M., Boudouresque, C., Enriquez, S., 2009. Seagrass ecosystems and Mediterranean seagrasses. Bot. Mar. 52, 369–381.
Saderne, V., Baldry, K., Anton, A., Agustí, S., Duarte, C.M., 2019. Characterization of the CO2 system in a coral reef, a seagrass meadow, and a mangrove forest in the central red sea. J. Geophys. Res.: Oceans 124, 7513–7528.
Santos, I.R., Burdige, D.J., Jennerjahn, T.C., Bouillon, S., Cabral, A., Serrano, O., Wernberg, T., Filbee-Dexter, K., Guimond, J.A., Tamborski, J.J., 2021. The renaissance of Odum's outwelling hypothesis in 'Blue Carbon' science. Estuar. Coast Shelf Sci. 255, 107361.
Santos, I.R., Maher, D.T., Eyre, B.D., 2012. Coupling automated radon and carbon dioxide measurements in coastal waters. Environ. Sci. Technol. 46, 7685–7691.
Santos, I.R., Maher, D.T., Larkin, R., Webb, J.R., Sanders, C.J., 2019. Carbon outwelling and outgassing vs. burial in an estuarine tidal creek surrounded by mangrove and saltmarsh wetlands. Limnol. Oceanogr. 64, 996–1013.
Schmidt, C., Hanfland, C., Regnier, P., Van Cappellen, P., Schluter, M., Knauthe, U., Stimac, I., Geibert, W., 2011. ^{228}Ra, ^{226}Ra, ^{224}Ra and ^{223}Ra in potential sources and sinks of land-derived material in the German Bight of the North Sea: implications for the use of radium as a tracer. Geo Mar. Lett. 31, 259–269.
Serrano, O., Mateo, M., Renom, P., 2011. Seasonal response of Posidonia oceanica to light disturbances. Mar. Ecol. Prog. Ser. 423, 29–38.
Serrano, O., Mateo, M., Renom, P., Julia Brugues, R., 2012. Characterization of soils beneath a Posidonia oceanica meadow. Geoderma s 185–186, 26–36.
Sippo, J.Z., Maher, D.T., Schulz, K.G., Sanders, C.J., McMahon, A., Tucker, J., Santos, I. R., 2019. Carbon outwelling across the shelf following a massive mangrove dieback in Australia: insights from radium isotopes. Geochem. Cosmochim. Acta 253, 142–158.
Tait, D.R., Santos, I.R., Erler, D.V., Befus, K.M., Cardenas, M.B., Eyre, B.D., 2013. Estimating submarine groundwater discharge in a South Pacific coral reef lagoon using different radioisotope and geophysical approaches. Mar. Chem. 156, 49–60.
Tamborski, J.J., Eagle, M., Kurylyk, B.L., Kroeger, K.D., Wang, Z.A., Henderson, P., Charette, M.A., 2021. Pore water exchange-driven inorganic carbon export from intertidal salt marshes. Limnol. Oceanogr. 66, 1774–1792.
Thomas, H., Schiettecatte, L.S., Suykens, K., Koné, Y.J.M., Shadwick, E.H., Prowe, A.E.F., Bozec, Y., de Baar, H.J.W., Borges, A.V., 2009. Enhanced ocean carbon storage from anaerobic alkalinity generation in coastal sediments. Biogeosciences 6, 267–274.
Tokoro, T., Hosokawa, S., Miyoshi, E., Tada, K., Watanabe, K., Montani, S., Kayanne, H., Kuwae, T., 2014. Net uptake of atmospheric CO_2 by coastal submerged aquatic vegetation. Global Change Biol. 20, 1873–1884.
Van Dam, B.R., Lopes, C., Osburn, C.L., Fourqurean, J.W., 2019. Net heterotrophy and carbonate dissolution in two subtropical seagrass meadows. Biogeosciences 16, 4411–4428.
Van Dam, B.R., Lopes, C.C., Polsenaere, P., Price, R.M., Rutgersson, A., Fourqurean, J.W., 2021a. Water temperature control on CO_2 flux and evaporation over a subtropical seagrass meadow revealed by atmospheric eddy covariance. Limnol. Oceanogr. 66, 510–527.
Van Dam, B.R., Zeller, M.A., Lopes, C., Smyth, A.R., Bottcher, M.E., Osburn, C.L., Zimmerman, T., Profrock, D., Fourqurean, J.W., Thomas, H., 2021b. Calcification-driven CO_2 emissions exceed "Blue Carbon"sequestration in a carbonate seagrass meadow. Sci. Adv. 7, eabj1372.
Venkiteswaran, J.J., Schiff, S.L., Wassenaar, L.I., 2008. Aquatic metabolism and ecosystme health assessment using dissolved O_2 stable isotope diel curves. Ecol. Appl. 18, 965–982.
Wanninkhof, R., 1992. Relationship between wind speed and gas exchange over the ocean. J. Geophys. Res.: Oceans 97, 7373–7382.
Wanninkhof, R., McGillis, W.R., 1999. A cubic relationship between air-sea CO_2 exchange and wind speed. Geophys. Res. Lett. 26, 1889–1892.
Yadav, V.B., Jha, S.K., 2019. Estimation of apparent water age and mixing process of water in the creek ecosystem of Mumbai Harbour Bay. Regional Studies in Marine Science 31, 100755.
Yau, Y.Y.Y., Xin, P., Chen, X., Zhan, L., Call, M., Conrad, S.R., Sanders, C.J., Li, L., Du, J., Santos, I.R., 2022. Alkalinity Export to the Ocean Is a Major Carbon Sequestration Mechanism in a Macrotidal Saltmarsh. Limnology and Oceanography n/a.
Zeebe, R.E., Wolf-Gladrow, D., 2001. CO2 in Seawater: Equilibrium, Kinetics, Isotopes. Gulf Professional Publishing.
Zhang, J.-Z., Fischer, C., 2014. Carbon Dynamics of Florida Bay: Spatiotemporal Patterns and Biological Control, vol. 48. Environmental science & technology.